Article

Optimization of CO_2/H_2 Separation over Ba-SAPO-34 Zeolite Membrane Synthesized by Microwave Heating

Tiffany Yit Siew Ng [1,2], Vinosha Viriya [1,2], Thiam Leng Chew [1,2,*], Yin Fong Yeong [1,2], Abdul Latif Ahmad [3], Chii-Dong Ho [4] and Zeinab Abbas Jawad [5]

[1] CO2 Research Centre (CO2RES), Institute of Contaminant Management, Universiti Teknologi PETRONAS, Seri Iskandar 32610, Perak, Malaysia
[2] Department of Chemical Engineering, Universiti Teknologi PETRONAS, Seri Iskandar 32610, Perak, Malaysia
[3] School of Chemical Engineering, Universiti Sains Malaysia, Nibong Tebal 14300, Penang, Malaysia
[4] Department of Chemical and Materials Engineering, Tamkang University, New Taipei City 25137, Taiwan
[5] Department of Chemical Engineering, College of Engineering, Qatar University, Doha P.O. Box 2713, Qatar
* Correspondence: thiamleng.chew@utp.edu.my

Abstract: CO_2/H_2 separation using membrane technology is an important research area in order to obtain high purity hydrogen as one source of clean energy. Finding a suitable inorganic membrane is one of the critical issues, which needs to be explored for CO_2/H_2 separation. In the present study, Ba-SAPO-34 zeolite membrane was synthesized and followed by a modification process. CO_2/H_2 separation of the membrane was investigated by varying the independent process variables (CO_2 % in the feed, pressure difference across the membrane and temperature). Modeling and optimization for the responses (CO_2/H_2 separation selectivity and CO_2 permeance) was performed by applying response surface methodology and central composite design, which is available in Design Expert software. The accuracy of the models in predicting the response was tested by comparing with the experimental value of response and the two values were in good agreement. The optimization of the models gave CO_2 permeance of 19.23×10^{-7} mol/m^2 s Pa and CO_2/H_2 separation selectivity of 11.6 at 5% CO_2 in the feed, a pressure difference of 100 kPa, and temperature of 30 °C for Ba-SAPO-34 zeolite membrane.

Keywords: zeolite membrane; Ba-SAPO-34; CO_2/H_2 separation; response surface methodology

1. Introduction

In recent years, gas separation has received enormous attention among researchers due to the issues of energy security and global climate change. Numbers of articles for gas separation processes have been published [1–5]. Hydrogen (H_2) separation technologies have gained increasing importance nowadays since hydrogen is one of the important chemical sources for industries. It is also one the main energy sources for transportation fuel and electrical power generation [6]. Separation and purification are important technologies in processes for H_2 production, such as thermochemical processes. In order to obtain high purity H_2, separation of H_2 from carbon dioxide (CO_2) is one such important area [5].

Common separation techniques for H_2 separation from CO_2 are physical absorption with solvents, pressure swing adsorption and cryogenic distillation [5,7]. However, these processes have a number of drawbacks such as complexity of the system, high energy consumption for solvent regeneration, equipment corrosion and flow problems caused by viscosity of solvent [8,9]. Membrane-based technology appears to be a potential alternative for H_2 separation in view of its advantages such as sustainable operation and relatively low energy consumption [7]. Palladium membranes have been extensively studied for H_2 separation due to its high hydrogen selectivity [10–12]. However, the usage of palladium and its alloys have a number of disadvantages, including a high sensitivity to chemicals (i.e., sulphur, chlorine and carbon monoxide in most applications) and their extremely

high cost [13]. Polymeric membrane are other candidates for separation of H_2 in view of their low cost and low energy requirement [14,15]. However, the application of polymeric membrane in H_2 separation is limited by the disadvantages such as the low mechanical stability of rubbery polymers [16].

Zeolite membranes are microporous inorganic membranes that are gaining increasing interests for CO_2/H_2 separation. Zeolite membranes possess advantages such as uniform pore structure and high chemical stability [17,18]. Different types of zeolite membranes have been studied for gas permeation and separation. These include CHA [17], FAU-type [19,20], PWN-type [21], A-type [22–25], MFI-type [26–31], DDR [32,33], T-type [34,35] and silicoaluminophosphate (SAPO) membranes [18,36,37]. There have been a number of studies on SAPO-34 zeolite membrane for gas permeation and separation due to its small pore structure [18,36–46]. Owing to the pore size of SAPO-34 which is close to the kinetic diameter of the CO_2 molecule, the SAPO-34 zeolite membrane has a high potential for separation of H_2 from CO_2. Hong et al. [39] reported that the SAPO-34 membrane selectively separated CO_2 from the CO_2/H_2 binary gas mixture at low temperature and the membrane became H_2 selective at a high temperature of 200 °C.

Design of Experiments is commonly used to perform optimization for the process parameters [47]. Response surface methodology (RSM), available in Design of Experiments, is a statistical tool that could allow reduction in the required numbers of experiments and could be used to investigate the effect of the significant process variable and the effect of the variables' interaction on the process [48]. There have been numerous studies that have applied RSM and hence showed RSM as an effective tool for optimization of the process [49–52].

Our previous work [53] has shown that CO_2/CH_4 separation was selectivity improved from 30 for the H-SAPO-34 zeolite membrane to 103 for the Ba-SAPO-34 zeolite membrane. In the present work, Ba-SAPO-34 zeolite membrane was formed by modifying the pre-synthesized H^+-form of SAPO-34 (H-SAPO-34) zeolite membrane. The Ba-SAPO-34 zeolite membrane was subjected to the CO_2/H_2 separation process by varying three process variables, which are CO_2 % (concentration) in the feed, pressure difference and temperature. The objective of the current study was to perform optimization on the operating process conditions of the membrane separation for the CO_2/H_2 separation selectivity and CO_2 permeance. In current work, CO_2 permeance was reported instead of H_2 permeance because the Ba-SAPO-34 membrane was found to be CO_2-selective over the ranges of the process variables studied.

2. Materials and Methods

2.1. Preparation of Zeolite Membrane

H-SAPO-34 membrane was deposited on α-alumina disc and then followed by a modification to the Ba-SAPO-34 membrane by following the procedures described in our previous work [43,53]. The synthesis precursor with the molar composition of $Al_2O_3:P_2O_5:1.2$TEAOH:$0.3SiO_2:80H_2O$ was prepared by mixing deionized water, aluminium isopropoxide ($Al(i\text{-}C_3H_7O)_3$, 98%, Merck, Darmstadt, Germany), tetraethylammonium hydroxide (TEAOH, 35 wt%, Sigma–Aldrich, St. Louis, MI, USA), phosphoric acid (H_3PO_4, 85%, Sigma–Aldrich) and Ludox AS-40 colloidal silica sol (40 wt%). The synthesis precursor was poured into a Teflon-lined vessel with α-Alumina disc placed in the vessel. The filled Teflon-lined vessel was heated at 200 °C for 2 h in a microwave oven (MARS 5, CEM Corporation, Matthews, NC, Canada). When the microwave heating was done, rinsing and drying were performed on the membrane. The procedures for heating, rinsing and drying were repeated three times. Calcination was performed on the H-SAPO-34 membrane at 400 °C for 15 h in a furnace. In order to modify the H-SAPO-34 membrane to the Ba-SAPO-34 membrane, ion-exchange was performed on the H-SAPO-34 membrane at 70 °C for 5 h by using ion-exchange solution containing Ba^{2+}. Rinsing the membrane with ethanol and followed by drying the membrane at 100 °C overnight were then carried out.

The characterization works of the Ba-SAPO-34 membrane were described in our previous work [43,53].

2.2. Design of Experiments

By using Design Expert software version 6.0.6 (STAT-EASE Inc., Minneapolis, MN, USA), Design of Experiments was applied for investigating the CO_2/H_2 separation. The modeling and analysis of problems, which include the generation of model equations by using experimental data, determination of the effect of variables and variables' interaction on the responses and optimization studies on the responses, were performed by using RSM coupled with central composite design (CCD) [54,55].

Three independent variables were studied for CO_2/H_2 separation in the current study, which include CO_2 % in the feed, pressure difference and temperature, as shown in Table 1. The factor code for CO_2 % in the feed, pressure difference and temperature is C, B and A, respectively. As shown in Table 1, the low level and high level are represented by −1 and +1, respectively. CO_2 separation selectivity and CO_2 permeance are the responses that were investigated in the current study.

Table 1. Independent variables with ranges for CO_2/H_2 separation studies in the current study.

Variable (Unit)	Level and Range		
	−1	0	+1
CO_2 % in the feed (%)	5.0	27.5	50.0
Pressure difference (kPa)	100	300	500
Temperature (°C)	30	105	180

Equations (1) and (2) show the polynomial that can be investigated by using Design Expert software for the approximation for the relationship between response (*y*) and the set of independent variables [50,54,56]:

First order model:

$$y = \beta_0 + \beta_1 x_1 + \beta_2 x_{2-} + \ldots + \beta_n x_n + \varepsilon \tag{1}$$

Second order model:

$$y = \beta_0 + \sum_{i=1}^{n} \beta_i x_i + \sum_{i=1}^{n} \beta_{ii} x_i^2 + \sum\sum_{i<j} \beta_{ij} x_i x_j + \varepsilon \tag{2}$$

where *y* is the response, x_i and x_j are the independent variables, $x_i x_j$ is the first order interaction between x_i and x_j, β_0, β_i, β_{ii} and β_{ij} is the regression coefficient for intercept, linear, quadratic and interaction terms, respectively, *n* is the number of independent variables and ε is the error.

2.3. CO_2/H_2 Gas Separation Studies

The Ba-SAPO-34 membrane was sealed in a stainless steel module using silicone gaskets and was subjected to CO_2/H_2 separation studies. Mass flow controllers were used to feed CO_2 and H_2 gases to the membrane module The CO_2 concentration in the feed was varied. The permeate pressure was kept at atmospheric pressure. Back pressure regulator was used to adjust the feed pressure so that the pressure difference across Ba-SAPO-34 membrane can be varied. The temperature for gas separation was varied by changing the temperature of an electronic-controlled oven where the membrane module was located. Online gas chromatography (PERKIN ELMER, CLARUS 500) equipped with CARBOXEN-1010 column and thermal conductivity detector, was used to analyze the composition of the permeate and retentate exit streams.

Permeance, P_i (mol/m^2 s Pa) of the gas was determined by using Equation (3).

$$P_i = \frac{J_i}{\Delta p_i} \tag{3}$$

where Δp_i is the partial pressure difference of gas i across the membrane (Pa), J_i is the flux of gas i (mol/m^2 s), the gas i may corresponds to CO_2 or H_2.

The CO_2/H_2 separation selectivity, α_{CO_2/H_2} was determined by using Equation (4).

$$\alpha_{CO_2/H_2} = \frac{P_{CO_2}}{P_{H_2}} \tag{4}$$

3. Results

3.1. Characterization Results of Ba-SAPO-34

The Ba-SAPO-34 membrane was characterized by using Scanning Electron Microscopy (SEM) and High-Resolution Transmission Electron Microscopy (HRTEM) in our previous work [43]. The top view SEM image and cross-sectional view SEM image of Ba-SAPO-34 membrane can be found in our previously published works [43]. It was observed from the top view SEM image of the Ba-SAPO-34 membrane that the membrane consists of orthorhombic zeolite crystals with a size of approximately 1 μm [43]. Meanwhile, the cross-sectional view SEM image of the Ba-SAPO-34 membrane showed that Ba-SAPO-34 membrane layer thickness is 4 μm approximately [43]. On the other hand, the HRTEM image of Ba-SAPO-34 can also be found in our previously published works [43] and the HRTEM showed Ba-SAPO-34 with pore channel diameter of less than 0.5 nm.

3.2. Experiment Design Matrix

In the current study, a total of 20 experiment runs for sets of independent variables (C: CO_2 % in the feed, B: pressure difference and A: temperature) was suggested by CCD for the CO_2/H_2 gas separation studies as shown in Table 2. The values of CO_2/H_2 separation selectivity and CO_2 permeance, which were obtained from experimental work, are shown in Table 2 as well. The CO_2 permeance was in the range of 1.96 to 19.23 $\times 10^{-7}$ mol/m^2 s Pa and the CO_2/H_2 separation selectivity was in the range of 2.3 to 12.2. The experimental runs at the temperature of 105 °C, pressure difference of 300 kPa and 27.5% CO_2 in the feed were repeated another five times (run 15–20 as shown in Table 2) in order to check for the reproducibility of the data. The low values of standard deviations (0.01 for CO_2 permeance and 0.05 for CO_2/H_2 separation selectivity) for the repeated runs indicates good reproducibility of the responses.

3.3. Response Surface Modeling

"Inverse" transformation was used to analyze the responses of CO_2 permeance and CO_2/H_2 separation selectivity as defined in Equation (5).

$$y\prime = \frac{1}{y} \tag{5}$$

where y is the value of the response and y' is the transformed value. "Inverse" transformation was applied because this function was able to model and predict the experimental data very well. The CO_2 permeance and CO_2/H_2 separation selectivity was modeled, analyzed in the form of 1/(CO_2 permeance) and 1/(CO/H_2 separation selectivity) respectively.

3.3.1. Response Surface Modeling of CO_2 Permeance

The Analysis of Variance (ANOVA) of the CO_2 permeance is shown in Table 3. Equation (6) shows the chosen quadratic model to reflect the relationship between the independent variables and the response.

$$1/(CO_2 \text{ Permenace}) = +0.30 + 0.051A + 0.037B + 0.14C + 0.017A^2 - 0.026B^2 \\ -0.018C^2 - 0.030AB + 0.026AC + 0.011BC \tag{6}$$

where C, B and A correspond to the coded value of CO_2 % in the feed, pressure difference and temperature, respectively.

Table 2. Independent variables and responses for the CO_2/H_2 separation studies.

Run	Variable			Response	
	A	**B**	**C**	**CO_2 Permeance ($\times 10^{-7}$ mol/m^2 s Pa)**	**CO_2/H_2 Separation Selectivity**
	Temperature (°C)	Pressure Difference (kPa)	CO_2 % in the Feed		
1	30	100	5	19.23	12.2
2	180	100	5	6.15	3.1
3	30	500	5	6.08	5.1
4	180	500	5	6.51	4.0
5	30	100	50	3.85	6.6
6	180	100	50	2.11	1.8
7	30	500	50	2.39	5.0
8	180	500	50	1.96	2.3
9	30	300	27.5	3.74	5.3
10	180	300	27.5	2.71	2.4
11	105	100	27.5	4.17	3.0
12	105	500	27.5	3.21	3.1
13	105	300	5	6.98	4.4
14	105	300	50	2.36	3.0
			Repeated Runs		
15	105	300	27.5	3.32	3.0
16	105	300	27.5	3.30	3.1
17	105	300	27.5	3.31	3.1
18	105	300	27.5	3.33	3.1
19	105	300	27.5	3.31	3.0
20	105	300	27.5	3.31	3.0
	Mean			3.31	3.05
	Standard Deviation			0.01	0.05

Table 3. ANOVA of the CO_2 permeance.

Source	Sum of Squares	Degree of Freedom	Mean Square	F Value	Prob > F
Model	0.260	9	0.029	29,876.61	<0.0001
A	0.026	1	0.026	26,945.27	<0.0001
B	0.014	1	0.014	14,341.69	<0.0001
C	0.200	1	0.200	20.81×10^{-6}	<0.0001
A^2	7.589×10^{-4}	1	7.589×10^{-4}	794.40	<0.0001
B^2	1.847×10^{-3}	1	1.847×10^{-3}	1932.97	<0.0001
C^2	8.992×10^{-4}	1	8.992×10^{-4}	941.26	<0.0001
AB	7.434×10^{-3}	1	7.434×10^{-3}	7781.67	<0.0001
AC	5.317×10^{-3}	1	5.317×10^{-3}	5566.44	<0.0001
BC	1.046×10^{-3}	1	1.046×10^{-3}	1094.58	<0.0001
Residual	9.553×10^{-6}	10	9.553×10^{-7}	-	-
Lack of Fit	5.140×10^{-6}	5	1.028×10^{-6}	1.16	0.4357
Pure Error	4.413×10^{-6}	5	8.826×10^{-7}	-	-
Cor Total	0.260	19	-	-	-

The model F-value of 29,876.61 implies the model was significant. Temperature (A) gave the highest F value of 26,945.27, indicating that it had the most significant effect on CO_2 permeance compared to pressure difference (B) and CO_2 % in the feed (C).

In order to have the terms of the model to be significant at the 95% confidence level, the values of probability should be less than 0.0500 ("Prob > F" less than 0.0500). In this case, all the terms (A, B, C, A^2, B^2, C^2, AB, AC and BC) were found to be significant for the model of $1/(CO_2$ permeance). The "Lack of Fit F-value" of 1.16 implied that the Lack of Fit was not significant relative to the pure error. It is good to have non-significant Lack of Fit.

Figure 1 presents the comparison between predicted $1/(CO_2$ permeance) attained by using Equation (6) with the experimental $1/(CO_2$ permeance). Good agreement between predicted $1/(CO_2$ permeance) and experimental $1/(CO_2$ permeance) is indicated by the correlation coefficient value (R^2) of 1.000. Hence, this reflects the high accuracy of the generated model Equation (6) to predict the $1/(CO_2$ permeance) in current work.
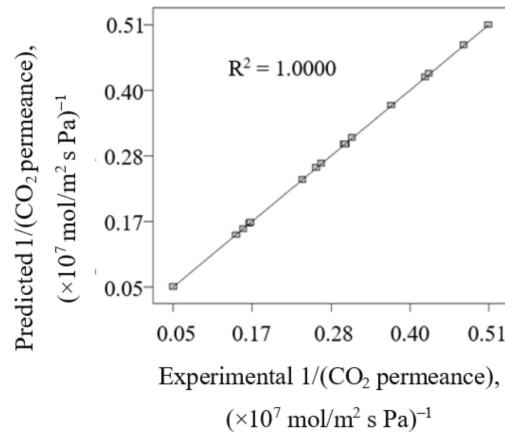

Figure 1. The comparison between predicted $1/(CO_2$ permeance) attained by using Equation (6) with the experimental $1/(CO_2$ permeance).

Figures 2–4 present the plots showing the effect of interaction between different independent variables on the $1/(CO_2$ permeance). It can be observed from Figure 2 that the $1/(CO_2$ permeance) increased with temperature for all three levels of pressure difference. A similar trend was reported by Li et al. [42]. When the separation temperature increased from 30 to 180 °C, the surface coverage declined and the CO_2 diffusivity increased. The decline in surface coverage prevailed the increment in diffusivity when the temperature increased. Subsequently, this resulted in decline in CO_2 permeance, and hence increment in the $1/(CO_2$ permeance) when the temperature increased. The $1/(CO_2$ permeance also increased with pressure difference as shown in Figure 2. In the current study, gas permeance was calculated by dividing the gas flux with partial pressure difference across the membrane. The increase in CO_2 partial pressure gradient was more than the increase in CO_2 surface coverage gradient, hence leading to a decrease in CO_2 permeance with an increase in pressure difference of 100–500 kPa across the membrane in the current study. Figures 3 and 4 show that the $1/(CO_2$ permeance) increased with an increase in CO_2 % in the feed from 5 to 50%. When the CO_2 % in the feed increased, the CO_2 permeance decreased. The increase in the CO_2 loading approached saturation in the membrane and thus resulted in drop in CO_2 permeance as observed and reported by Hong et al. [39].
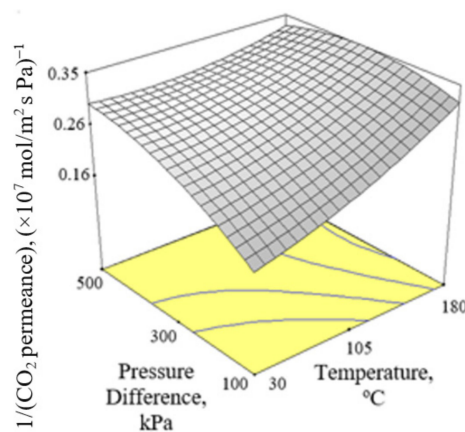

Figure 2. Effect of interaction between temperature and pressure difference on the $1/(CO_2$ permeance) at 27.5% CO_2 in the feed.
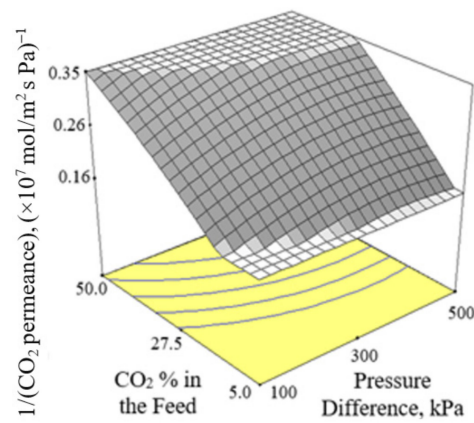
Figure 3. Effect of interaction between CO_2 % in the feed and pressure difference on the $1/(CO_2$ permeance) at 105 °C.
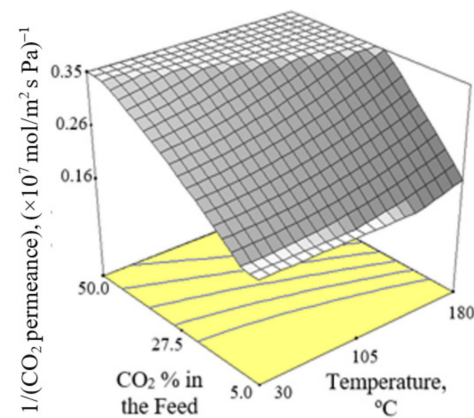

Figure 4. Effect of interaction between CO_2 % in the feed and temperature on the $1/(CO_2$ permeance) at 300 kPa pressure difference.

3.3.2. Response Surface Modeling of CO_2/H_2 Separation Selectivity

The ANOVA of the CO_2/H_2 separation selectivity is shown in Table 4. Equation (7) shows the chosen quadratic model to reflect the relationship between the independent variables and the response.

$$
\begin{aligned}
1/(CO_2/H_2 \text{ Separation Selectivity}) = {} & +0.32 + 0.12A - 0.005579B + 0.060C - 0.020A^2 \\
& +0.010B^2 - 0.039C^2 - 0.046AB + 0.043AC \\
& -0.015BC
\end{aligned}
\tag{7}
$$

where C, B and A correspond to the coded value of CO_2 % in the feed, pressure difference and temperature, respectively.

The model was significant in view of its F-value of 391.84. The significance of variable's effect on CO_2/H_2 separation selectivity decreased in the order of temperature (A) > CO_2 % in the feed (C) > pressure difference (B) with the F-value in the order of 2209.94 > 586.84 > 5.03, respectively. It is shown in Table 4 that A, B, C, A^2, C^2, AB, AC, BC were significant terms for the model of $1/(CO_2/H_2$ separation selectivity). However, the term of B^2 was included in Equation (7) to obtain a hierarchy model. The "Lack of Fit F-value" of 4.39 implied that the Lack of Fit was not significant relative to the pure error due to noise.

Figure 5 presents the comparison of the predicted $1/(CO_2/H_2$ separation selectivity) attained by using Equation (7) with the experimental $1/(CO_2/H_2$ separation selectivity). Good agreement between predicted $1/(CO_2/H_2$ separation selectivity) and experimental $1/(CO_2/H_2$ separation selectivity) is indicated by the correlation coefficient value (R^2) of 0.9972. Hence, this reflects the high accuracy of the generated model Equation (7) to predict the $1/(CO_2/H_2$ separation selectivity) in the current work.

Table 4. ANOVA of CO_2/H_2 separation selectivity.

Source	Sum of Squares	Degree of Freedom	Mean Square	F Value	Prob > F
Model	0.220	9	0.024	391.84	<0.0001
A	0.140	1	0.140	2209.94	<0.0001
B	3.112×10^{-4}	1	3.112×10^{-4}	5.03	0.0488
C	0.036	1	0.036	586.84	<0.0001
A^2	1.156×10^{-3}	1	1.156×10^{-3}	18.68	0.0015
B^2	2.755×10^{-4}	1	2.755×10^{-4}	4.45	0.0610
C^2	4.118×10^{-3}	1	4.118×10^{-3}	66.57	<0.0001
AB	0.017	1	0.017	269.22	<0.0001
AC	0.015	1	0.015	243.05	<0.0001
BC	1.851×10^{-3}	1	1.851×10^{-3}	29.93	0.0003
Residual	6.186×10^{-4}	10	6.186×10^{-5}	-	-
Lack of Fit	5.036×10^{-4}	5	1.007×10^{-4}	4.39	0.0655
Pure Error	1.150×10^{-4}	5	2.300×10^{-5}	-	-
Cor Total	0.220	19	-	-	-

Figures 6–8 present the plots showing the effect of interaction between different independent variables on the $1/(CO_2/H_2$ separation selectivity). It is shown in Figure 6 that the $1/(CO_2/H_2$ separation selectivity) increased when the temperature increased from 30 to 180 °C. CO_2 adsorbed more strongly on Ba-SAPO-34 membrane than H_2, and hence permeated faster through the membrane pore despite its larger molecule kinetic diameter than H_2 [57]. Therefore, the CO_2/H_2 separation selectivities obtained in the current study were more than 1. The values became less than 1 when the CO_2/H_2 separation selectivities were inversed. At temperature as low as 30 °C, strong CO_2 adsorption on the membrane inhibited the adsorption and permeance of H_2. The degree of CO_2 inhibition toward H_2 adsorption reduced due to lower CO_2 surface coverage when the temperature increased [39]. The CO_2 permeance decreased but the H_2 permeance increased, led to a drop in CO_2/H_2 separation selectivity or in other words, an increase in $1/(CO_2/H_2$ separation selectivity) when the temperature increased. When the CO_2 % in the feed increased, the $1/(CO_2/H_2$ separation selectivity) increased, as can be seen in Figures 7 and 8.
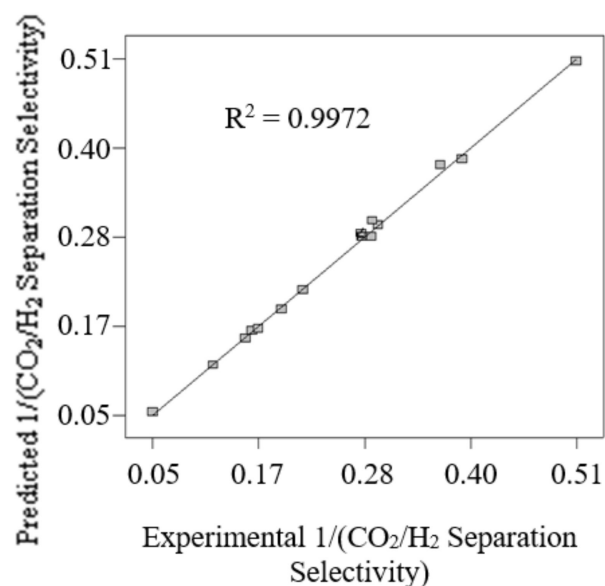

Figure 5. The comparison of the predicted $1/(CO_2/H_2$ separation selectivity) attained by using Equation (7) with the experimental $1/(CO_2/H_2$ separation selectivity).

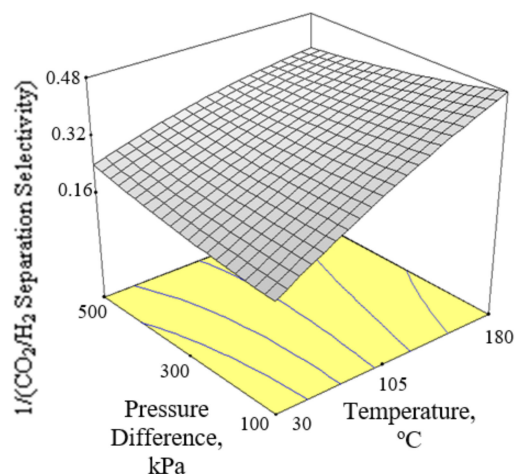**Figure 6.** Effect of interaction between temperature and pressure difference on the $1/(CO_2/H_2$ separation selectivity) at 27.5% CO_2 in the feed.
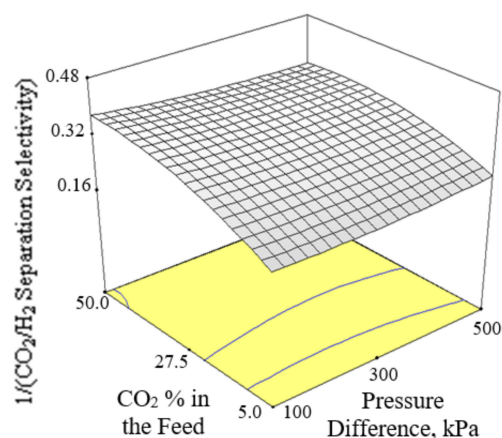

Figure 7. Effect of interaction between CO_2 % in the feed and pressure difference on the $1/(CO_2/H_2$ separation selectivity) at 105 °C.
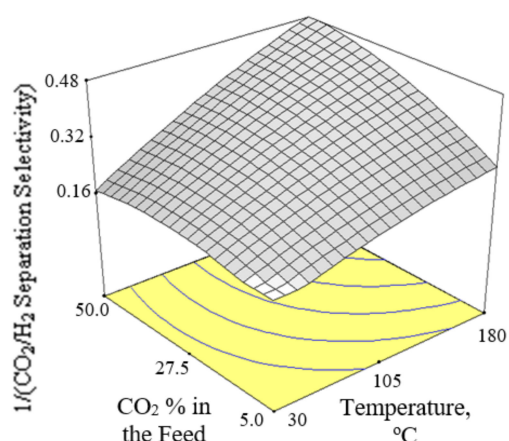

Figure 8. Effect of interaction between CO_2 % in the feed and temperature on the $1/(CO_2/H_2$ separation selectivity) at 300 kPa pressure difference.

3.4. Optimization Studies

The goal set for the responses and variables, that need to be satisfied simultaneously for optimizing the responses by using Design Expert, is presented in Table 5. It was the goal for the responses to minimize the $1/(CO_2/H_2$ separation selectivity) and the $1(CO_2$

permeance), or in other words, to maximize the CO_2/H_2 separation selectivity and the CO_2 permeance.

Table 5. Goal set for optimization of the studies of CO_2/H_2 separation.

	Name	Goal	Lower Limit	Upper Limit
Variable	Temperature, °C	Within range	30	100
	Pressure Difference, kPa	Within range	100	500
	CO_2 % in the Feed	Within range	5	50
Response	1/(CO_2 Permeance), $(\times 10^{-7}\ \mathrm{mol/m^2\ s\ Pa})^{-1}$	Minimum	0.05	0.51
	1/(CO_2/H_2 Separation Selectivity)	Minimum	0.08	0.56

Design Expert generated solutions (optimum conditions) with different total desirability as shown in Table 6. The desirability function approach was applied in the RSM to optimize the operating conditions in the present work.

Table 6. Optimum conditions for the 1/(CO_2/H_2 separation selectivity) and the 1/(CO_2 permeance) generated by Design Expert.

Solu-tion	Temperature, °C	Pressure Difference, kPa	CO_2 % in the Feed	1/(CO_2 Permeance), $(\times 10^{-7}\ \mathrm{mol/m^2\ s\ Pa})^{-1}$	1/(CO_2/H_2 Separation Selectivity)	Total Desirability
1	30.00	100.00	5.00	0.052	0.086	0.996
2	30.00	100.00	5.35	0.056	0.087	0.990
3	30.01	107.02	5.00	0.056	0.087	0.990
4	30.07	114.32	5.00	0.060	0.088	0.985
5	30.00	102.66	6.03	0.060	0.091	0.982
6	31.91	100.00	5.93	0.059	0.094	0.980
7	40.46	100.00	5.00	0.056	0.107	0.969

This approach was applied to determine the operating condition that results in response to the highest desirability. Each estimated response variable was transformed into an individual desirability value, d_i, using the desirability function [58]. The value of the desirability varies over the range

$$0 \leq d_i \leq 1 \tag{8}$$

where (d_i = 1) reflects a completely ideal response value and (d_i = 0) reflects a completely undesirable response value. Then, the individual desirability values were combined in order to determine the value of the total desirability, D, as shown in Equation (9).

$$D = (d_1 \times d_2 \times \ldots \times d_m)^{\frac{1}{m}} \tag{9}$$

where m is the number of responses. In view of the highest total desirability of 0.996 displayed by Solution 1 as shown in Table 6. Solution 1 was selected as the optimum condition. With the optimum condition of Solution 1, 1/(CO_2/H_2 separation selectivity) value of 0.086 and the 1/(CO_2 permeance) value of 0.052 $(\times 10^{-7}\ \mathrm{mol/m^2\ s\ Pa})^{-1}$, were attained, which are equivalent to CO_2/H_2 separation selectivity of 11.6 and CO_2 permeance of $19.23 \times 10^{-7}\ \mathrm{mol/m^2\ s\ Pa}$.

An additional five experiments were conducted at the optimum operating condition (temperature of 30 °C, pressure difference of 100 kPa, 5% CO_2 in the feed) generated by Design of Experiments in order to check the accuracy of the Design of Experiments. The separation result is presented in Table 7. The experimental values of CO_2/H_2 separation selectivity and CO_2 permeance were compared with the values predicted by using the models. The attainment of mean error of 3.64% for CO_2/H_2 separation selectivity and the

mean error of 1.46% for CO_2 permeance reflects good agreement between the predicted values and the experimental values. This implies that Design of Experiments with RSM is an accurate tool used to model and predict CO_2/H_2 separation performance of the membrane in the current work.

Table 7. The results of the additional CO_2/H_2 separation experiments conducted at optimum operating condition generated by Design of Experiments.

Run	CO₂ Permeance ($\times 10^{-7}$ mol/m² s Pa)		ΔError (%)	CO₂/H₂ Separation Selectivity		ΔError (%)
	Experimental	Predicted (Design of Experiments)		Experimental	Predicted (Design of Experiments)	
1	19.11	19.23	0.62	12.1	11.6	4.13
2	18.99	19.23	1.25	11.9	11.6	2.52
3	19.01	19.23	1.14	12.2	11.6	4.92
4	19.52	19.23	1.51	12.2	11.6	4.92
5	18.70	19.23	2.76	11.8	11.6	1.69
Mean Error			1.46			3.64
Standard Deviation			0.71			1.31

3.5. Comparison of CO_2/H_2 Separation Performance with the Other Zeolite Membranes Reported in the Literature

The Ba-SAPO-34 zeolite membrane in the present study was also compared for its CO_2/H_2 gas separation performance with the other zeolite membranes reported in the literature, and the comparison is shown in Table 8. Yin et al. [59] prepared a stainless-steel-net-supported P/NaX composite, which displayed CO_2/H_2 selectivity of ~4.1–6.4 and CO_2 permeance of ~0.18–1.68 $\times 10^{-7}$ mol/m² s Pa. Mirfendereski et al. [60] reported H_2/CO_2 selectivity of 0.11–0.22, which is equivalent to CO_2/H_2 selectivity of ~9.1–4.5 for ZSM-5 zeolite membranes. In the other studies reported by Aydani et al. [61], the SSZ-13 membrane was synthesized by dynamic rub coating. CO_2 permeance of 5.8×10^{-7} mol/m² s Pa and CO_2/H_2 selectivity of 17 were obtained for the synthesized SSZ-13 membrane [61]. On the other hand, CO_2/H_2 selectivity of 17 was reported for the DDR membrane by Zito et al. [62].

Table 8. Comparison of CO_2/H_2 separation performance with the other zeolite membranes reported in the literature.

Zeolite Membrane	CO₂/H₂ Selectivity * or H₂/CO₂ Separation Factor +	Reference
Ba-SAPO-34	1.8–12.2 *	Present study
P/NaX	~4.1–6.4 *	[59]
ZSM-5	~9.1–4.5 *	[60]
SSZ-13	17 *	[61]
DDR	17 *	[62]
Na-LTA	5.9 +	[63]
Cs-LTA	8 +	[63]
AlPO₄-LTA	7.3 +	[64]

* CO_2/H_2 Selectivity; + H_2/CO_2 Separation Factor.

Xu et al. [63] prepared Na-LTA and Cs-LTA membranes. Xu et al. [63] reported an H_2/CO_2 separation factor of 5.9 and 8 for Na-LTA and Cs-LTA membranes, respectively. Moreover, Li et al. [64] reported the synthesis of the AlPO₄-LTA membrane and obtained an H_2/CO_2 separation factor of 7.3 for the AlPO₄-LTA membrane. The reported H_2/CO_2

separation factor values of greater than one for these membranes indicates that these membranes are H_2-selective.

4. Conclusions

In this study, the CO_2/H_2 separation process over Ba-SAPO-34 zeolite membrane was investigated. Modeling and optimization for the responses (CO_2/H_2 separation selectivity and CO_2 permeance) as a function of the independent process variables (CO_2 % in the feed, pressure difference and temperature) was performed by applying response surface methodology and central composite design, which is available in Design Expert software. The obtained model equations were able to predict the responses over the ranges of CO_2 % in the feed, pressure difference and temperature studied. In addition, optimum CO_2 permeance of 19.23×10^{-7} mol/m^2 s Pa and CO_2/H_2 separation selectivity of 11.6 were obtained at 5% CO_2 in the feed, pressure difference of 100 kPa and temperature of 30 °C for the Ba-SAPO-34 zeolite membrane.

Author Contributions: Conceptualization, T.L.C.; methodology, T.L.C.; validation, T.L.C.; formal analysis, T.L.C.; investigation, T.L.C.; writing—original draft preparation, T.L.C.; writing—review and editing, T.Y.S.N., V.V. and Y.F.Y.; visualization, C.-D.H. and Z.A.J.; supervision, A.L.A. All authors have read and agreed to the published version of the manuscript.

Conflicts of Interest: The authors declare no conflict of interest. The funders had no role in the design of the study; in the collection, analyses, or interpretation of data; in the writing of the manuscript; or in the decision to publish the results.

References

1. Ismail, A.F.; David, L.I.B. A review on the latest development of carbon membranes for gas separatio. *J. Membr. Sci.* **2001**, *193*, 1–18. [CrossRef]
2. Yang, H.; Xu, Z.; Fan, M.; Gupta, R.; Slimane, R.B.; Bland, A.E.; Wright, I. Progress in carbon dioxide separation and capture: A review. *J. Environ. Sci.* **2008**, *20*, 14–27. [CrossRef]
3. Koros, W.J.; Mahajan, R. Pushing the limits on possibilities for large scale gas separation: Which strategies? *J. Membr. Sci.* **2000**, *175*, 181–196. [CrossRef]
4. Adhikari, S.; Fernando, S. Hydrogen Membrane Separation Techniques. *Ind. Eng. Chem. Res.* **2006**, *45*, 875–881. [CrossRef]
5. Lu, G.Q.; Diniz da Costa, J.C.; Duke, M.; Giessler, S.; Socolow, R.; Williams, R.H.; Kreutz, T. Inorganic membranes for hydrogen production and purification: A critical review and perspective. *J. Colloid Interface Sci.* **2007**, *314*, 589–603. [CrossRef]
6. Moon, J.-H.; Bae, J.-H.; Han, Y.-J.; Lee, C.-H. Adsorbent/membrane hybrid (AMH) system for hydrogen separation: Synergy effect between zeolite 5A and silica membrane. *J. Membr. Sci.* **2010**, *356*, 58–69. [CrossRef]
7. Bai, X.; Shi, Z.; Xia, H.; Li, S.; Liu, Z.; Liang, H.; Liu, Z.; Wang, B.; Qiao, Z. Machine-Learning-Assisted High-Throughput computational screening of Metal—Organic framework membranes for hydrogen separation. *Chem. Eng. J.* **2022**, *446*, 136783. [CrossRef]
8. Gray, M.L.; Soong, Y.; Champagne, K.J.; Pennline, H.; Baltrus, J.P.; Stevens, R.W., Jr.; Khatri, R.; Chuang, S.S.C.; Filburn, T. Improved immobilized carbon dioxide capture sorbents. *Fuel Proc. Technol.* **2005**, *86*, 1449–1455. [CrossRef]
9. Zheng, F.; Tran, D.N.; Busche, B.J.; Fryxell, G.E.; Addleman, R.S.; Zemanian, T.S.; Aardahl, C.L. Ethylenediamine-modified SBA-15 as regenerable CO_2 sorbent. *Ind. Eng. Chem. Res.* **2005**, *44*, 3099–3105. [CrossRef]

10. David, E.; Kopac, J. Devlopment of palladium/ceramic membranes for hydrogen separation. *Int. J. Hydrogen Energy* **2011**, *36*, 4498–4506. [CrossRef]

11. Shi, L.; Goldbach, A.; Xu, H. High-flux H_2 separation membranes from (Pd/Au)n nanolayers. *Int. J. Hydrogen Energy* **2011**, *36*, 2281–2284. [CrossRef]

12. Nagata, K.; Miyamoto, M.; Watabe, T.; Fujioka, Y.; Yogo, K. Preparation of pore-fill-type palladium-porous alumina composite membrane for hydrogen separation. *Chem. Lett.* **2011**, *40*, 19–21. [CrossRef]

13. Li, X.; Zhou, C.; Lin, Z.; Rocha, J.; Lito, P.F.; Santiago, A.S.; Silva, C.M. Titanosilicate AM-3 membrane: A new potential candidate for H_2 separation. *Microporous Mesoporous Mater.* **2011**, *137*, 43–48. [CrossRef]

14. Lin, H.; Freeman, B.D. Gas permeation and diffusion in cross-linked poly(ethylene glycol) diacrylate). *Macromolecules* **2006**, *39*, 3568–3580. [CrossRef]

15. Lin, H.; Van Wagner, E.; Freeman, B.D.; Toy, L.G.; Gupta, R.P. Plasticization-enhanced hydrogen purification using polymeric membranes. *Science* **2006**, *311*, 639–642. [CrossRef]

16. Iqbal, Z.; Shamair, Z.; Usman, M.; Gilani, M.A.; Yasin, M.; Saqib, S.; Khan, A.L. One pot synthesis of UiO-66@IL composite for fabrication of CO_2 selective mixed matrix membranes. *Chemosphere* **2022**, *303*, 135122. [CrossRef] [PubMed]

17. Zhou, J.; Wu, S.; Liu, B.; Zhou, R.; Xing, W. Scalable fabrication of highly selective SSZ-13 membranes on 19-channel monolithic supports for efficient CO_2 capture. *Sep. Purif. Technol.* **2022**, *293*, 121122. [CrossRef]

18. Wang, B.; Huang, W.; Zhu, Y.; Zhou, R.; Xing, W. Ultra-permeable high-selective SAPO-34 membranes for efficient CO_2 capture. *J. Membr. Sci.* **2022**, *650*, 120420. [CrossRef]

19. Gu, X.; Dong, J.; Nenoff, T.M. Synthesis of defect-free FAU-type zeolite membranes and separation for dry and moist CO_2/N_2 mixtures. *Ind. Eng. Chem. Res.* **2005**, *44*, 937–944. [CrossRef]

20. Sato, K.; Sugimoto, K.; Sekine, Y.; Takada, M.; Matsukata, M.; Nakane, T. Application of FAU-type zeolite membranes to vapor/gas separation under high pressure and high temperature up to 5 MPa and 180 °C. *Microporous Mesoporous Mater.* **2007**, *101*, 312–318. [CrossRef]

21. Mohammadzadeh, M.; Pakdel, S.; Azamat, J.; Erfan-Niya, H.; Khataee, A. Theoretical Study of CO_2/N_2 Gas Mixture Separation through a High-Silica PWN-type Zeolite Membrane. *Ind. Eng. Chem. Res.* **2022**, *61*, 5593–5599. [CrossRef]

22. Nishiyama, N.; Yamaguchi, M.; Katayama, T.; Hirota, Y.; Miyamoto, M.; Egashira, Y.; Ueyama, K.; Nakanishi, K.; Ohta, T.; Mizusawa, A.; et al. Hydrogen-permeable membranes composed of zeolite nano-blocks. *J. Membr. Sci.* **2007**, *306*, 349–354. [CrossRef]

23. Li, Y.; Chen, H.; Liu, J.; Yang, W. Microwave synthesis of LTA zeolite membranes without seeding. *J. Membr. Sci.* **2006**, *277*, 230–239. [CrossRef]

24. Das, N.; Kundu, D.; Chatterjee, M. The effect of intermediate layer on synthesis and gas permeation properties of NaA zeolite membrane. *J. Coat. Technol. Res.* **2010**, *7*, 383–390. [CrossRef]

25. Xu, X.; Yang, W.; Liu, J.; Lin, L.; Stroh, N.; Brunner, H. Synthesis of NaA zeolite membrane on a ceramic hollow fiber. *J. Membr. Sci.* **2004**, *229*, 81–85. [CrossRef]

26. Sebastián, V.; Kumakiri, I.; Bredesen, R.; Menéndez, M. Zeolite membrane for CO_2 removal: Operating at high pressure. *J. Membr. Sci.* **2007**, *292*, 92–97. [CrossRef]

27. Mabande, G.T.P.; Noack, M.; Avhale, A.; Kölsch, P.; Georgi, G.; Schwieger, W.; Caro, J. Permeation properties of bi-layered Al-ZSM-5/Silicalite-1 membranes. *Microporous Mesoporous Mater.* **2007**, *98*, 55–61. [CrossRef]

28. Bernal, M.P.; Coronas, J.; Menéndez, M.; Santamaría, J. Separation of CO_2/N_2 mixtures using MFI-type zeolite membranes. *AIChE J.* **2004**, *50*, 127–135. [CrossRef]

29. Piera, E.; Brenninkmeijer, C.A.M.; Santamaría, J.; Coronas, J. Separation of traces of CO from air using MFI-type zeolite membranes. *J. Membr. Sci.* **2002**, *201*, 229–232. [CrossRef]

30. Poshusta, J.C.; Noble, R.D.; Falconer, J.L. Temperature and pressure effects on CO_2 and CH_4 permeation through MFI zeolite membranes. *J. Membr. Sci.* **1999**, *160*, 115–125. [CrossRef]

31. Shin, D.W.; Hyun, S.H.; Cho, C.H.; Han, M.H. Synthesis and CO_2/N_2 gas permeation characteristics of ZSM-5 zeolite membranes. *Microporous Mesoporous Mater.* **2005**, *85*, 313–323. [CrossRef]

32. Himeno, S.; Tomita, T.; Suzuki, K.; Nakayama, K.; Yajima, K.; Yoshida, S. Synthesis and permeation properties of a DDR-type zeolite membrane for separation of CO_2/CH_4 gaseous mixtures. *Ind. Eng. Chem. Res.* **2007**, *46*, 6989–6997. [CrossRef]

33. Tomita, T.; Nakayama, K.; Sakai, H. Gas separation characteristics of DDR type zeolite membrane. *Microporous Mesoporous Mater.* **2004**, *68*, 71–75. [CrossRef]

34. Mirfendereski, S.M.; Mazaheri, T.; Sadrzadeh, M.; Mohammadi, T. CO_2 and CH_4 permeation through T-type zeolite membranes: Effect of synthesis parameters and feed pressure. *Sep. Purif. Technol.* **2008**, *61*, 317–323. [CrossRef]

35. Cui, Y.; Kita, H.; Okamoto, K.-i. Preparation and gas separation performance of zeolite T membrane. *J. Mater. Chem.* **2004**, *14*, 924–932. [CrossRef]

36. Li, S.; Carreon, M.A.; Zhang, Y.; Funke, H.H.; Noble, R.D.; Falconer, J.L. Scale-up of SAPO-34 membranes for CO_2/CH_4 separation. *J. Membr. Sci.* **2010**, *352*, 7–13. [CrossRef]

37. Li, S.; Fan, C.Q. High-flux SAPO-34 membrane for CO_2/N_2 separation. *Ind. Eng. Chem. Res.* **2010**, *49*, 4399–4404. [CrossRef]

38. Hong, M.; Li, S.; Funke, H.F.; Falconer, J.L.; Noble, R.D. Ion-exchanged SAPO-34 membranes for light gas separations. *Microporous Mesoporous Mater.* **2007**, *106*, 140–146. [CrossRef]

39. Hong, M.; Li, S.; Falconer, J.L.; Noble, R.D. Hydrogen purification using a SAPO-34 membrane. *J. Membr. Sci.* **2008**, *307*, 277–283. [CrossRef]

40. Li, S.; Alvarado, G.; Noble, R.D.; Falconer, J.L. Effects of impurities on CO_2/CH_4 separations through SAPO-34 membranes. *J. Membr. Sci.* **2005**, *251*, 59–66. [CrossRef]

41. Li, S.; Martinek, J.G.; Falconer, J.L.; Noble, R.D.; Gardner, T.Q. High-pressure CO_2/CH_4 separation using SAPO-34 membranes. *Ind. Eng. Chem. Res.* **2005**, *44*, 3220–3228. [CrossRef]

42. Li, S.; Falconer, J.L.; Noble, R.D. SAPO-34 membranes for CO_2/CH_4 separations: Effect of Si/Al ratio. *Microporous Mesoporous Mater.* **2008**, *110*, 310–317. [CrossRef]

43. Chew, T.L.; Yeong, Y.F.; Ho, C.D.; Ahmad, A.L. Ion-Exchanged Silicoaluminophosphate-34 Membrane for Efficient CO_2/N_2 Separation with Low CO_2 Concentration in the Gas Mixture. *Ind. Eng. Chem. Res.* **2019**, *58*, 729–735. [CrossRef]

44. Tian, Y.; Fan, L.; Wang, Z.; Qiu, S.; Zhu, G. Synthesis of a SAPO-34 membrane on macroporous supports for high permeance separation of a CO_2/CH_4 mixture. *J. Mater. Chem.* **2009**, *19*, 7698–7703. [CrossRef]

45. Falconer, J.L.; Carreon, M.A.; Li, S.; Noble, R.D. Synthesis of zeolites and zeolite membranes using multiple structure directing agents. U.S. Patent No. 8,302,782, 2012, 18 September 2008.

46. Carreon, M.A.; Li, S.; Falconer, J.L.; Noble, R.D. SAPO-34 seeds and membranes prepared using multiple structure directing agents. *Adv. Mater.* **2008**, *20*, 729–732. [CrossRef]

47. Tong, L.-I.; Chang, Y.-C.; Lin, S.-H. Determining the optimal re-sampling strategy for a classification model with imbalanced data using design of experiments and response surface methodologies. *Expert Syst. Appl.* **2011**, *38*, 4222–4227. [CrossRef]

48. Vicente, G.; Martínez, M.; Aracil, J. Optimisation of integrated biodiesel production. Part I. A study of the biodiesel purity and yield. *Biores. Technol.* **2007**, *98*, 1724–1733. [CrossRef] [PubMed]

49. Fan, M.-S.; Abdullah, A.Z.; Bhatia, S. Hydrogen production from carbon dioxide reforming of methane over Ni-Co/MgO-ZrO₂ catalyst: Process optimization. *Int. J. Hydrogen Energy* **2011**, *36*, 4875–4886. [CrossRef]

50. Sun, Y.; Xu, W.; Zhang, W.; Hu, Q.; Zeng, X. Optimizing the extraction of phenolic antioxidants from kudingcha made frrom Ilex kudingcha C.J. Tseng by using response surface methodology. *Sep. Purif. Technol.* **2011**, *78*, 311–320. [CrossRef]

51. Low, K.L.; Tan, S.H.; Zein, S.H.S.; McPhail, D.S.; Boccaccini, A.R. Optimization of the mechanical properties of calcium phosphate/multi-walled carbon nanotubes/bovine serum albumin composites using response surface methodology. *Mater. Des.* **2011**, *32*, 3312–3319. [CrossRef]

52. Switzar, L.; Giera, M.; Lingeman, H.; Irth, H.; Niessen, W.M.A. Protein digestion optimization for characterization of drug-protein adducts using response surface modeling. *J. Chromatogr. A* **2011**, *1218*, 1715–1723. [CrossRef] [PubMed]

53. Chew, T.L.; Ahmad, A.L.; Bhatia, S. Ba-SAPO-34 membrane synthesized from microwave heating and its performance for CO_2/CH_4 gas separation. *Chem. Eng. J.* **2011**, *171*, 1053–1059. [CrossRef]

54. Montgomery, D.C. *Design and Analysis of Experiments*, 7th ed.; John Wiley & Sons, Inc.: Hoboken, NJ, USA, 2009.

55. Yeong, Y.F.; Abdullah, A.Z.; Ahmad, A.L.; Bhatia, S. Process optimization studies of p-xylene separation from binary xylene mixture over silicalite-1 membrane using response surface methodology. *J. Membr. Sci.* **2009**, *341*, 96–108. [CrossRef]

56. Wee, S.L.; Tye, C.T.; Bhatia, S. Process optimization studies for the dehydration of alcohol-water system by inorganic membrane based pervaporation separation using design of experiments (DOE). *Sep. Purif. Technol.* **2010**, *71*, 192–199. [CrossRef]

57. Hong, M.; Falconer, J.L.; Noble, R.D. Modification of zeolite membranes for H_2 separation by catalytic cracking of methyldiethoxysilane. *Ind. Eng. Chem. Res.* **2005**, *44*, 4035–4041. [CrossRef]

58. Derringer, G.; Suich, R. Simultaneous optimization of several response variables. *J. Qual. Technol.* **1980**, *12*, 214–219. [CrossRef]

59. Yin, X.; Zhu, G.; Wang, Z.; Yue, N.; Qiu, S. Zeolite P/NaX composite membrane for gas separation. *Microporous Mesoporous Mater.* **2007**, *105*, 156–162. [CrossRef]

60. Mirfendereski, S.M.; Mazaheri, T. Preparation of high performance ZSM-5 zeolite membranes for CO_2/H_2 separation. *J. Ind. Eng. Chem.* **2021**, *94*, 240–252. [CrossRef]

61. Aydani, A.; Brunetti, A.; Maghsoudi, H.; Barbieri, G. CO_2 separation from binary mixtures of CH_4, N_2, and H_2 by using SSZ-13 zeolite membrane. *Sep. Purif. Technol.* **2021**, *256*, 117796. [CrossRef]

62. Zito, P.F.; Brunetti, A.; Drioli, E.; Barbieri, G. CO_2 Separation via a DDR Membrane: Mutual Influence of Mixed Gas Permeation. *Ind. Eng. Chem. Res.* **2020**, *59*, 7054–7060. [CrossRef]

63. Xu, C.; Wei, W.; He, Y. Enhanced hydrogen separation performance of Linde Type-A zeolite molecular sieving membrane by cesium ion exchange. *Mater. Lett.* **2022**, *324*, 132680. [CrossRef]

64. Li, L.; Li, X.; Wang, B.; Zi, W.; Ji, Q.; Li, Y.; Zhang, X.; Wang, Y.; Ding, Y.; Liu, J.; et al. Ultrafast synthesis of discrete submicron AlPO₄-LTA molecular sieve crystals and their application in molecular sieve membrane. *Microporous Mesoporous Mater.* **2022**, *334*, 111771. [CrossRef]